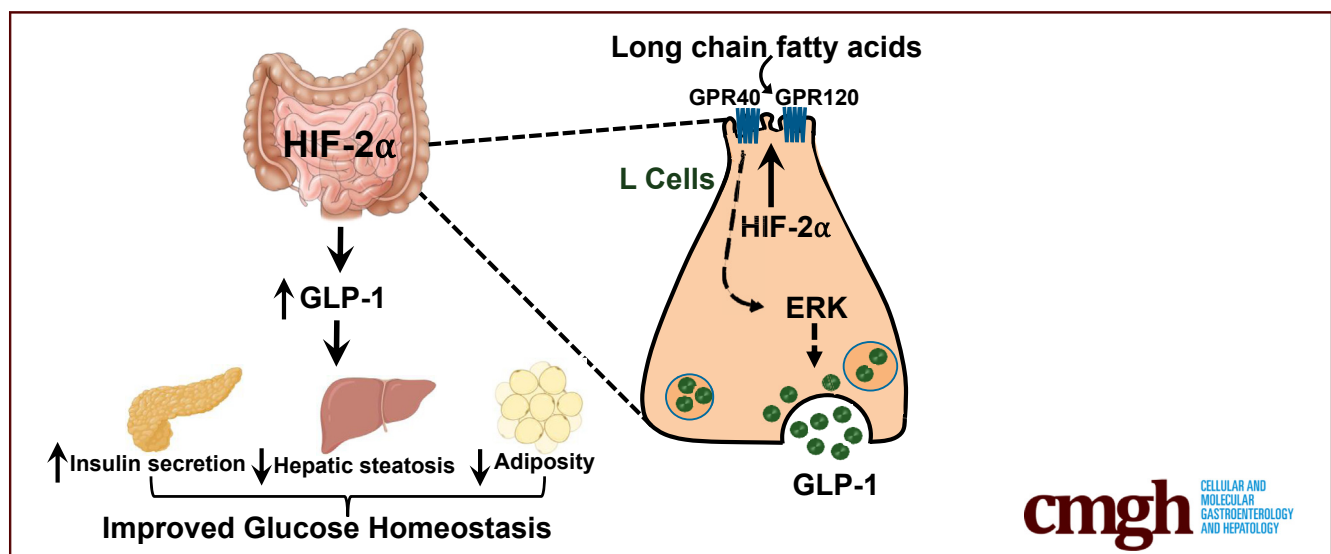


ORIGINAL RESEARCH

Intestinal HIF-2 α Regulates GLP-1 Secretion via Lipid Sensing in L-Cells

Raja Gopal Reddy Mooli,¹ Dhanunjay Mukhi,¹ Anil K. Pasupulati,¹ Simon S. Evers,² Ian J. Sipula,¹ Michael Jurczak,¹ Randy J. Seeley,² Yatrik M. Shah,^{3,4} and Sadeesh K. Ramakrishnan¹

¹Division of Endocrinology and Metabolism, Department of Medicine, University of Pittsburgh, Pittsburgh, Pennsylvania; ²Department of Surgery, ³Department of Molecular and Integrative Physiology, ⁴Department of Internal Medicine, University of Michigan, Ann Arbor, Michigan



SUMMARY

Activation of intestinal hypoxia-inducible factor signaling improves glucose homeostasis in a glucagon-like peptide-1-dependent manner. We show that activation of intestinal hypoxia-inducible factor 2 α signaling increases GLP-1 levels and attenuates diet-induced metabolic perturbations such as visceral adiposity, glucose intolerance, and hepatic steatosis.

BACKGROUND & AIMS: Compelling evidence shows that glucagon-like peptide-1 (GLP-1) has a profound effect in restoring normoglycemia in type 2 diabetic patients by increasing pancreatic insulin secretion. Although L-cells are the primary source of circulating GLP-1, the current therapies do not target L-cells to increase GLP-1 levels. Our study aimed to determine the molecular underpinnings of GLP-1 secretion as an impetus to identify new interventions to target endogenous L-cells.

METHODS: We used genetic mouse models of intestine-specific overexpression of hypoxia-inducible factor (HIF)-1 α and HIF-2 α (*Vhl* ^{Δ IE}), conditional overexpression of intestinal HIF-2 α (*Hif-2 α* ^{L^{SL};Vilⁱⁿ-Cre/ERT2}), and intestine-specific HIF-2 α knockout

mice (*Hif-2 α* ^{Δ IE}) to show that HIF signaling, especially HIF-2 α , regulates GLP-1 secretion.

RESULTS: Our data show that intestinal HIF signaling improved glucose homeostasis in a GLP-1-dependent manner. Intestinal HIF potentiated GLP-1 secretion via the lipid sensor G-protein-coupled receptor (GPR)40 enriched in L-cells. We show that HIF-2 α regulates GPR40 in L-cells and potentiates fatty acid-induced GLP-1 secretion via extracellular regulated kinase (ERK). Using a genetic model of intestine-specific overexpression of HIF-2 α , we show that HIF-2 α is sufficient to increase GLP-1 levels and attenuate diet-induced metabolic perturbations such as visceral adiposity, glucose intolerance, and hepatic steatosis. Lastly, we show that intestinal HIF-2 α signaling acts as a priming mechanism crucial for postprandial lipid-mediated GLP-1 secretion. Thus, disruption of intestinal HIF-2 α decreases GLP-1 secretion.

CONCLUSIONS: In summary, we show that intestinal HIF signaling, particularly HIF-2 α , regulates the lipid sensor GPR40, which is crucial for the lipid-mediated GLP-1 secretion, and suggest that HIF-2 α is a potential target to induce endogenous GLP-1 secretion. (*Cell Mol Gastroenterol Hepatol* 2022;13:1057–1072; <https://doi.org/10.1016/j.jcmgh.2021.12.004>)

Keywords: GLP-1; L-Cells; HIF-2 α ; GPR40; Nutrient-Sensing.

The intestine plays a crucial yet complex role in integrating the nutrient inputs with central and peripheral metabolic homeostasis via gut-derived molecules.¹ Among them, gut-derived hormone glucagon-like peptide-1 (GLP-1) inhibits food intake and glucagon secretion, promotes pancreatic insulin secretion, and restores glycemia.^{2–4} Thus, GLP-1-based therapies, which include GLP-1 agonists and inhibitors of GLP-1 degrading enzymes, have a profound effect in ameliorating hyperglycemia in type 2 diabetes. However, these therapies do not target endogenous GLP-1 production largely owing to the incomplete understanding of the molecular underpinnings of the GLP-1 secretory mechanisms.

GLP-1 is secreted from L-cells of the intestine in response to nutrients such as monosaccharides and lipids via distinct mechanisms. For instance, glucose and fructose stimulate GLP-1 secretion by depolarizing the L-cells, whereas lipids, especially long-chain fatty acids (LCFAs), potently stimulate GLP-1 via G-protein-coupled receptor (GPR)40 and GPR120 enriched in the L-cells.^{4–8} Compelling evidence has shown that inhibition of GPR40/120 signaling impairs GLP-1 secretion and induces glucose intolerance, suggesting a crucial role for intestinal lipid-sensing in metabolic homeostasis.^{9–11} However, the mechanisms that regulate L-cell lipid-sensing are not well understood.

Under physiological conditions, the epithelial cells adjacent to the lumen have significantly lower oxygen tension than the base of the crypts. Thus, a steep oxygen gradient exists within intestinal villi and along the intestinal tract and is crucial for intestinal homeostasis.^{12–14} The intestinal oxygen levels are regulated by blood circulation, oxygen perfusion, and the metabolic activity of the epithelia.¹⁵ For instance, intestinal blood circulation is decreased at fasting, and refeeding induces intestinal hyperemia.^{12,16} In addition, mucosa experiences a uniquely steep gradient because of its juxtaposition with the anoxic lumen of the gut. The disruption in the intestinal oxygen gradient results in barrier dysfunction and colonization of pathogens, leading to inflammatory diseases.^{17–19} Thus, intestinal oxygen levels are dynamically regulated by nutritional cues; however, its metabolic relevance remains to be elucidated.

The hypoxic response is mediated by the transcription factors hypoxia-inducible factor (HIF)-1 α and HIF-2 α .^{20,21} Under normoxic conditions, HIF- α is hydroxylated at the proline residues by the prolyl hydroxylase domain (PHD) enzymes using the available molecular oxygen. The E3 ubiquitin ligase von-Hippel Lindau (VHL) then binds the hydroxylated HIF- α and induces its degradation. Under hypoxic conditions, HIF- α is no longer hydroxylated by PHD, resulting in its stabilization. HIF- α then heterodimerizes with the aryl hydrocarbon receptor nuclear translocator to induce the transcription of its target genes.²¹ HIF-1 α and HIF-2 α share several metabolic genes and also regulate a distinct set of genes. For instance, HIF-1 α regulates glycolytic genes, whereas HIF-2 α regulates the genes involved in lipid metabolism.²⁰ Given that intestinal glucose and lipid

metabolism regulate GLP-1 secretion,^{22,23} we hypothesized that intestinal HIF signaling could be involved in regulating GLP-1.

To date, intestinal HIF signaling has been investigated extensively in various diseases such as obesity, iron overload, inflammation, and cancer.^{24–26} We show a novel role of intestinal HIF, particularly HIF-2 α , in inducing the expression of the L-cell lipid-sensor GPR40. Mechanistically, we identify that HIF-2 α -GPR40 signaling promotes GLP-1 secretion via extracellular regulated kinase (ERK). We show that intestinal HIF-2 α in mice increases GPR40 expression, increases GLP-1 levels, and improves glucose tolerance. We further show the physiological relevance of intestinal HIF-2 α signaling in postprandial GLP-1 secretion and diet-induced metabolic syndrome. In summary, we provide empiric evidence that HIF-2 α could be a novel target to induce endogenous GLP-1 secretion by enhancing L-cell lipid-sensing.

Results

Intestinal HIF Signaling Improved Glucose Homeostasis via Incretin GLP-1

To determine if metabolic cues regulate intestinal hypoxia signaling, we assessed HIF-oxygen-dependent degradation (ODD) reporter mice that possess the ODD domain of HIF fused with luciferase, allowing visualization of HIF stabilization (Figure 1A). We found that fasting stabilized HIF in the small intestines as shown by increased luciferase activity (Figure 1B). Moreover, protein levels of Hif-1 α and Hif-2 α (Figure 1C) and their target genes such as *Dmt1*, *Dcytb*, *Glut1*, and *Pgk1* were increased significantly in the small intestines of fasted mice (Figure 1D), suggesting that metabolic cues activate HIF signaling in the intestine. To investigate whether intestinal hypoxia signaling has a metabolic role, we assessed mice with constitutive activation of intestinal-epithelial HIF generated by villin-Cre-mediated disruption of VHL (*Vhl* ^{Δ IE}). Our data show that *Vhl* ^{Δ IE} mice have lower body weight than wild-type littermate controls (Figure 1E). Although no difference in basal glucose levels was noticed, the intraperitoneal (IP) glucose tolerance test showed better glucose disposal in *Vhl* ^{Δ IE} mice (Figure 1F). Intriguingly, no difference in the

Abbreviations used in this paper: α -LA, α -linolenic acid; cDNA, complementary DNA; DMEM, Dulbecco's modified Eagle medium; DMOG, dimethylxalyl glycine; ERK, Extracellular signal Regulated Kinase; GLP-1, glucagon-like peptide-1; GPR, G-protein-coupled receptor; GSK, GSK1120212; HFD, high-fat diet; HIF, hypoxia-inducible factor; IP, intraperitoneal; LCFA, long-chain fatty acid; MEK, Mitogen-activated Protein Kinase; mRNA, messenger RNA; ODD, oxygen-dependent degradation; PBS, phosphate-buffered saline; pERK, Phospho Extracellular regulated kinase; PHD, prolyl hydroxylase domain; PKA, protein kinase A; qPCR, quantitative polymerase chain reaction; STC-1, Secretin tumor cell line-1; Vco₂, carbon dioxide production; VHL, von-Hippel Lindau; Vo₂, oxygen consumption.

 Most current article

© 2021 The Authors. Published by Elsevier Inc. on behalf of the AGA Institute. This is an open access article under the CC BY-NC-ND license (<http://creativecommons.org/licenses/by-nc-nd/4.0/>).

2352-345X

<https://doi.org/10.1016/j.jcmgh.2021.12.004>

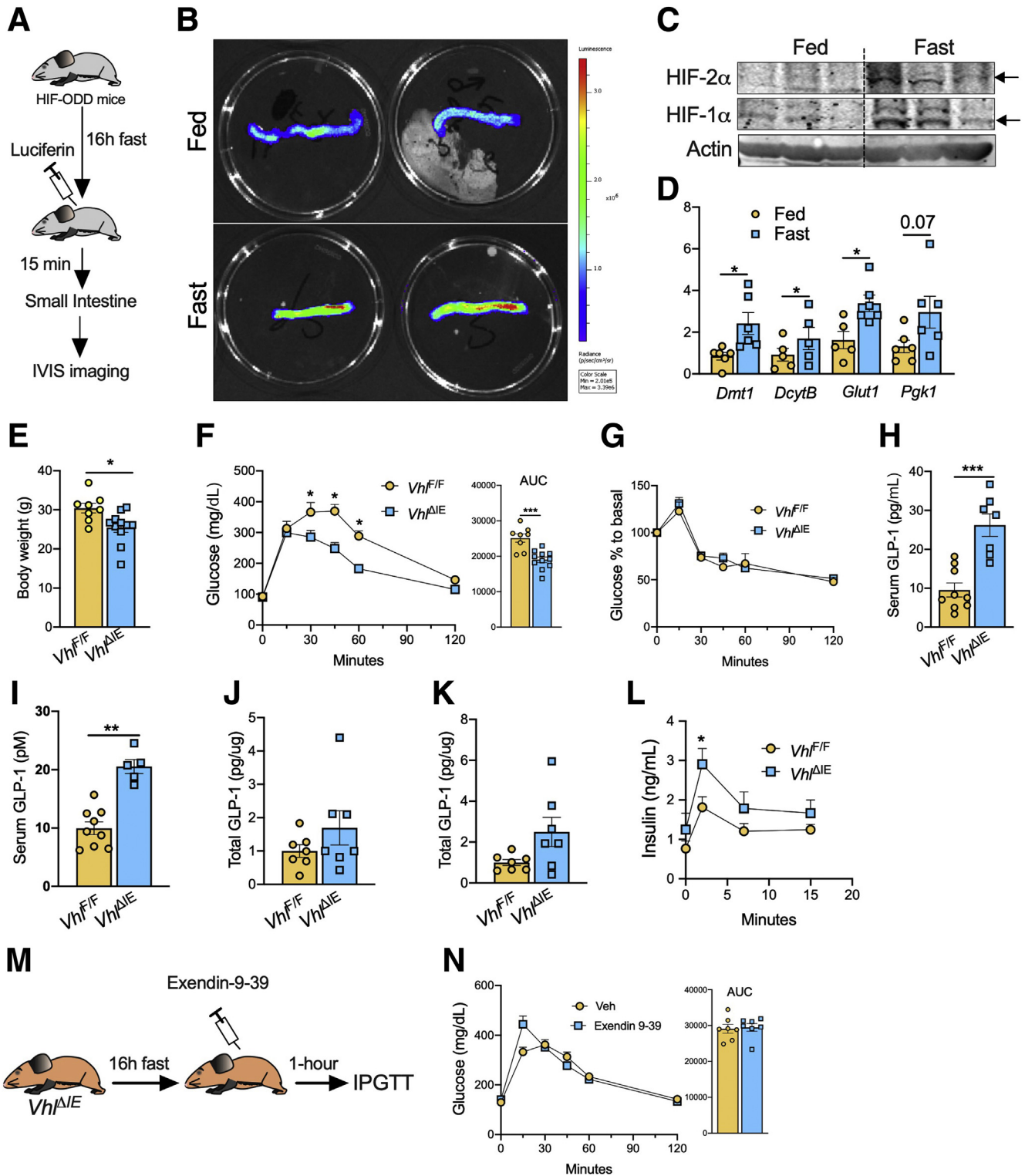


Figure 1. Activation of intestinal HIF signaling improves glucose homeostasis via GLP-1. (A) Schematic representation showing HIF-ODD mice assessed for luciferase activity after 16 hours of fasting. (B) IVIS imaging showing luciferase activity in the small intestine of HIF-ODD mice. *n* = 2 per group. (C) Western blot analysis in the ileal scrapes of C57BL/6 mice that were fasted for 16 hours. *n* = 3 mice per group. (D) qPCR analysis for HIF target genes in the small intestine of C57BL6 mice fasted for 16 hours. (E) Body weight of male *Vh^{ΔIE}* mice on a chow diet. (F) intraperitoneal glucose tolerance test (IPGTT) and (G) insulin tolerance test (ITT) in male *Vh^{ΔIE}* mice on a chow diet. Steady-state total serum GLP-1 assessed in (H) male and (I) female *Vh^{ΔIE}* mice. Total GLP-1 in the (J) ileum and (K) pancreas of *Vh^{ΔIE}* mice. (L) Glucose-stimulated insulin secretion in *Vh^{ΔIE}* mice. *n* = 4–5 mice per group. (M) Experimental schema and (N) glucose excursion during IPGTT performed 1 hour after administration of GLP-1 antagonist exendin 9-39. All data presented as means ± SEM. **P* ≤ .05, ***P* ≤ .01, and ****P* ≤ .001 as analyzed by 2-tailed Student *t* test.

insulin tolerance test mice was observed (Figure 1G), suggesting that intestinal HIF signaling improves glucose homeostasis independent of insulin sensitivity.

The intestine regulates systemic glucose homeostasis partially via the incretin GLP-1, which enhances glucose-stimulated insulin secretion from the pancreas.^{27,28} GLP-1-secreting L-cells are mostly scattered in the distal parts of the intestine,²⁹ where hypoxia is prevalent¹⁵; therefore, we assessed the possible role of intestinal HIF in regulating GLP-1. Remarkably, steady-state GLP-1 levels were increased significantly in male and female *Vhl*^{ΔIE} mice (Figure 1H and I). However, ileal and pancreatic total GLP-1 levels were unchanged (Figure 1J and K). The insulinotropic effect of GLP-1 was observed when glucose was administered orally.^{4,30} Because GLP-1 is increased at a steady-state, we hypothesized that IP glucose would potentiate glucose-stimulated insulin secretion in *Vhl*^{ΔIE} mice. Consistently, we found IP glucose challenge augmented first-phase insulin secretion in *Vhl*^{ΔIE} mice (Figure 1L). We then tested whether GLP-1 mediates the improvement in glucose homeostasis in *Vhl*^{ΔIE} mice. Administration of GLP-1 antagonists exendin 9-39 (Figure 1M) abolished the improvement in glucose tolerance in *Vhl*^{ΔIE} mice (Figure 1N), suggesting that intestinal HIF promotes systemic glucose homeostasis via GLP-1.

HIF Induces GLP-1 by Augmenting GPR40-Mediated Lipid Sensing

Because HIF-mediated transcriptional reprogramming promotes cellular differentiation,^{31,32} we assessed whether intestinal HIF induced L-cell differentiation. To this end, we performed immunostaining for GLP-1 in the small intestine, which showed no difference in the L-cell number between *Vhl*^{ΔIE} mice and littermate controls (Figure 2A). Quantitative polymerase chain reaction (qPCR) analysis in the small intestines of *Vhl*^{ΔIE} mice showed an increase in the messenger RNA (mRNA) levels of *Pcsk1*, which cleaves proglucagon (*Gcg*) to GLP-1 (Figure 2B). However, no difference in *Gcg* and *ChgA* mRNA levels were noted between the groups (Figure 2B), suggesting that L-cell content is not increased in *Vhl*^{ΔIE} mice. An increase in GLP-1 without changes in L-cell number indicated a potential involvement of secretory mechanisms. GLP-1 is secreted in response to luminal nutrients such as carbohydrates, lipids, and proteins.^{4,6} Our data show that *Vhl*^{ΔIE} mice had increased mRNA levels of *Glut1* (glucose metabolism), G-protein-coupled receptor (*Gpr*)40, and *Gpr120* (LCFA receptors). However, no difference in the amino acid sensor *Gpr142* was observed (Figure 2C). Thus, we posited that enhanced enteroendocrine glucose or lipid response could have increased GLP-1 levels in *Vhl*^{ΔIE} mice. We gavaged *Vhl*^{ΔIE} mice with glucose to test our hypothesis, which did not elicit any significant GLP-1 response (Figure 2D). However, LCFA-rich corn oil increased GLP-1 secretion in *Vhl*^{ΔIE} mice (Figure 2E), suggesting that intestinal HIF induces GLP-1 by augmenting L-cell lipid-sensing. LCFA stimulates GLP-1 secretion predominantly through GPR40, but not GPR120,³³ and, therefore, we tested whether GPR40 mediates intestinal HIF regulation of GLP-1 (Figure 2F). Our data

show that inhibition of GPR40 using a GPR40-specific antagonist, GW1100, did not affect GLP-1 levels in *Vhl*^{F/F} mice. Remarkably, GW1100 significantly reduced GLP-1 in *Vhl*^{ΔIE} mice (Figure 2G). Moreover, inhibition of GPR40 abolished the improvement in glucose tolerance in *Vhl*^{ΔIE} mice (Figure 2H), indicating that lipid sensing via GPR40 is necessary for HIF-mediated GLP-1 secretion and improvement in glucose homeostasis.

ERK Is the Downstream Target of HIF-2 α -GPR40 Signaling

Studies have shown that protein kinase A (PKA) mediates nutrient-stimulated GLP-1 secretion.^{34,35} However, we did not observe any induction in PKA signaling as assessed by phospho-PKA substrate levels in the small intestine of *Vhl*^{ΔIE} mice (Figure 2J). To identify the potential downstream mediators, we treated the enteroendocrine L-cell line (secretin tumor cell; STC-1) with ω -3 fatty acid α -linolenic acid (α -LA), the potent inducer of GLP-1. Consistent with previous studies,^{7,36} α -LA induced pERK levels in STC-1 cells (Figure 2J), and inhibition of ERK using the mitogen-activated protein-extracellular regulated kinase (MEK-ERK) inhibitor GSK1120212 (GSK) attenuated α -LA-induced GLP-1 secretion (Figure 2K), suggesting that lipid sensing stimulates GLP-1 via ERK. When we assessed the small intestine of *Vhl*^{ΔIE} mice, we found increased levels of pERK (Figure 2L), which was enhanced further in the ileal explants by α -LA treatment (Figure 2M). To determine whether HIF signaling regulates GLP-1 via ERK, we inhibited ERK using GSK (Figure 2N and O), which led to a significant reduction in GLP-1 levels in *Vhl*^{ΔIE} mice (Figure 2P). Further analysis showed that ERK inhibition did not affect *Gpr40* mRNA levels in *Vhl*^{ΔIE} mice (Figure 2Q), suggesting that ERK is downstream of GPR40 in HIF regulation of GLP-1 secretion.

Intestinal HIF-2 α Augments Lipid-Sensing and GLP-1 Secretion in L-Cells

HIF-1 α and HIF-2 α share several target genes and regulate a unique set of genes in a cell-specific manner.^{24,37} To characterize the isoform of HIF involved in lipid sensing, we transiently overexpressed HIF-1 α or HIF-2 α in STC-1 cells. HIF-1 α overexpression did not significantly change *Gpr40* and *Gpr120* mRNA levels (Figure 3A and B). However, HIF-2 α overexpression significantly induced both *Gpr40* and *Gpr120* mRNA levels (Figure 3C and D), with no change in the expression of *Pcsk1*, *Gcg*, and *ChgA* (Figure 3E). We then tested whether HIF-2 α overexpression would augment α -LA-induced GLP-1 secretion. Overexpression of HIF-2 α does not affect GLP-1 levels or pERK levels in the absence of ligand (Figure 3F and G). However, adding α -LA significantly increased GLP-1 levels and pERK in STC-1 cells overexpressing HIF-2 α (Figure 3G and H).

We then tested whether pharmacologic induction of HIF-2 α using dimethylxalyl glycine (DMOG) would augment the expression of lipid-sensing genes and GLP-1 secretion. DMOG-treated mice showed increased mRNA levels of HIF-2 α target genes and *Gpr40* and *Gpr120* in the small intestine

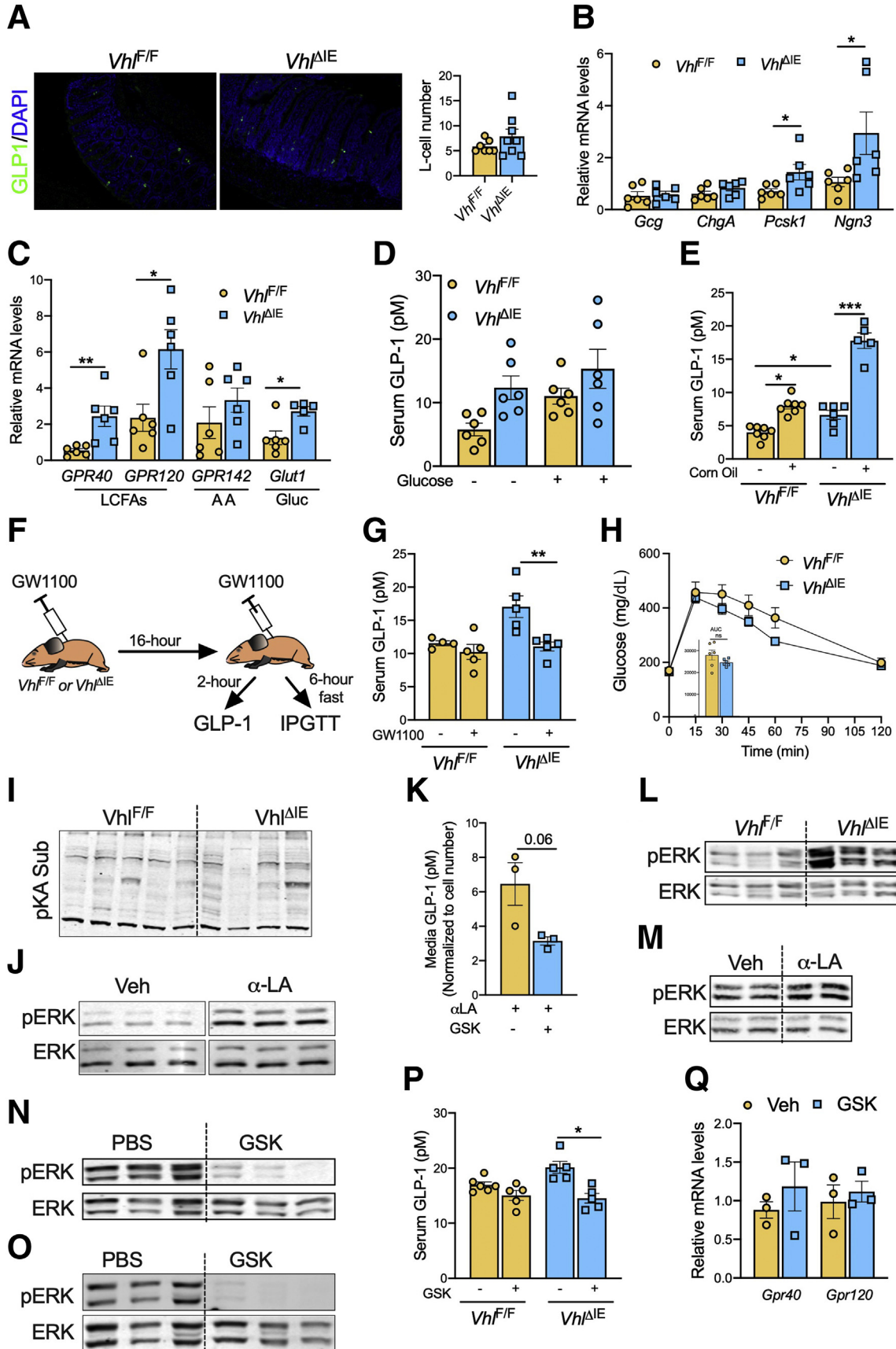


(Figure 3J). Furthermore, corn oil-stimulated GLP-1 secretion was potentiated in DMOG-treated mice (Figure 3J). Collectively, our data suggest that HIF-2 α promotes lipid-mediated GLP-1 secretion in L-cells.

We then tested whether intestinal HIF-2 α is sufficient to potentiate lipid sensing using mice with conditional overexpression of intestinal HIF-2 α (*Hif-2 α ^{LSL;Vil-in-Cre/ERT2}*) generated by crossing the mice with HIF-2 α driven by Rosa 26 flanked by locus of X-over P (loxP)-stop-loxP sites (*Hif-2 α ^{LSL}*), with mice expressing tamoxifen-inducible Cre recombinase driven under villin promoter (Figure 3K–M). Our data show that the temporal induction of HIF-2 α increases the mRNA levels of *Gpr40* and *Gpr120* in the small intestine of *Hif-2 α ^{LSL;Vil-in-Cre/ERT2}* mice (Figure 3N). Moreover, GLP-1 and pERK levels were increased in the intestines of *Hif-2 α ^{LSL;Vil-in-Cre/ERT2}* mice (Figure 3O and P). Thus, our data suggest that activation of intestinal HIF-2 α is sufficient to induce lipid-sensing genes and GLP-1. We then assessed whether intestinal HIF-2 α promotes metabolic homeostasis. A glucose tolerance test in chow-fed, tamoxifen-treated *Hif-2 α ^{LSL;Vil-in-Cre/ERT2}* mice showed improved glucose tolerance, albeit no difference in body weight (Figure 3Q and R), indicating that intestinal HIF-2 α promotes glucose homeostasis.

Intestinal HIF-2 α Attenuates Diet-Induced Glucose Intolerance

We then assessed if activation of intestinal HIF-2 α would ameliorate diet-induced glucose intolerance. To this end, *Hif-2 α ^{LSL}* and *Hif-2 α ^{LSL;Vil-in-Cre/ERT2}* mice were treated with tamoxifen to temporally activate HIF-2 α and then fed with a 60% high-fat diet (HFD) for 24 weeks (Figure 4A). *Hif-2 α ^{LSL;Vil-in-Cre/ERT2}* mice showed a significant decrease in body weight gain (Figure 4B), which was further evident from a significant reduction in fat mass along with an increase in lean mass (Figure 4C). The weight differences were not attributed to any change in intestinal lipid absorption (Figure 4D). However, the cumulative food intake assessed for 3 days was significantly lower in *Hif-2 α ^{LSL;Vil-in-Cre/ERT2}* mice (Figure 4E). Furthermore, the glucose tolerance test showed better glucose tolerance in *Hif-2 α ^{LSL;Vil-in-Cre/ERT2}* mice (Figure 4F), independent of insulin sensitivity (Figure 4G). These metabolic effects were associated with increased serum and ileal GLP-1 levels in HFD *Hif-2 α ^{LSL;Vil-in-Cre/ERT2}* mice (Figure 4H and I). qPCR analysis in

the small intestine showed a significant increase in *Pcsk1* and *Gcg*, albeit no change in L-cell number (Figure 4J and K). Furthermore, mRNA levels of *Gpr120* and *Gpr40* and pERK were increased in the small intestines of HFD *Hif-2 α ^{LSL;Vil-in-Cre/ERT2}* mice (Figure 4L and M). Thus, the data suggest that activation of intestinal HIF-2 α ameliorates diet-induced glucose intolerance and increases GPR40 signaling and GLP-1 levels.

Intestinal HIF-2 α Protects Against Diet-Induced Obesity and Hepatic Steatosis

To determine if intestinal HIF-2 α regulates energy homeostasis, we assessed *Hif-2 α ^{LSL;Vil-in-Cre/ERT2}* mice using indirect calorimetry. We found no difference in energy expenditure in HFD *Hif-2 α ^{LSL;Vil-in-Cre/ERT2}* mice (Figure 5A), or in oxygen consumption (V_{O_2}) or carbon dioxide production (V_{CO_2}) (Figure 5B). Despite the lack of changes in V_{CO_2} and V_{O_2} , we found a small but significant reduction in the ratio of V_{CO_2} to V_{O_2} , or the respiratory exchange ratio, in *Hif-2 α ^{LSL;Vil-in-Cre/ERT2}* mice (Figure 5C), indicating increased relative utilization of fat compared with carbohydrate metabolism. Assessment of gonadal adipose tissue showed decreased adiposity and adipocyte size in *Hif-2 α ^{LSL;Vil-in-Cre/ERT2}* mice (Figure 5D and E), which corroborated with increased lipolysis, as shown by increased phospho-hormone-sensitive lipase levels (Figure 5F). However, there was no change in adipose tissue inflammation (Figure 5G). Despite no difference in the liver weight (Figure 5H), we found a significant reduction in hepatic steatosis as shown by H&E analysis and lower hepatic triglyceride levels in HFD-fed *Hif-2 α ^{LSL;Vil-in-Cre/ERT2}* mice (Figure 5I and J). qPCR analysis in the livers of *Hif-2 α ^{LSL;Vil-in-Cre/ERT2}* mice showed a significant decrease in lipogenic genes such as *Cd36*, *Fasn*, *Srebp1c*, and *Plin2* (Figure 5K). However, no difference in fatty acid oxidation and inflammatory genes was noted, except *Acot1* and *Tnfa* (Figure 5K). Thus, although the mechanism behind the increase in relative whole-body fat utilization could not be accounted for by changes in hepatic gene expression, our data suggest that an increased supply of fatty acids resulting from increased lipolysis (Figure 5F) contributed to the effect via a substrate-driven mechanism that would provide more fatty acids to the liver, heart, brown adipose tissue (BAT), and skeletal muscle for oxidation. Collectively, our data show that activation of intestinal HIF-2 α attenuates visceral adiposity and hepatic steatosis.

Figure 2. (See previous page). Intestinal HIF promotes lipid-induced GLP-1 secretion via ERK. (A) Immunostaining for GLP-1 and L-cell number in the small intestine of *Vhl^{ΔIE}* mice. qPCR analysis for (B) enteroendocrine L-cell-specific genes and (C) nutrient-sensing/metabolism genes in the small intestines of *Vhl^{ΔIE}* mice. (D) Serum total GLP-1 levels assessed in *Vhl^{ΔIE}* mice gavaged with glucose (2 g/kg body weight), and blood was collected after 30 minutes. (E) Serum total GLP-1 levels in *Vhl^{ΔIE}* mice gavaged with corn oil (20 mL/kg body weight), and blood was collected after 30 minutes. (F) Experimental schema showing *Vhl^{ΔIE}* mice gavaged with GPR40 antagonist GW1100 at 2.5 mg/kg body weight at the indicated time points. (G) Serum total GLP-1 levels and (H) blood glucose excursion and area under curve (AUC) during intraperitoneal glucose tolerance test (ipGTT) in GW100-treated mice. (I) Western blot for phospho protein kinase A (pPKA) substrate in the small intestine of *Vhl^{ΔIE}* mice. (J) Western blot analysis in STC-1 cells treated with 50 μ mol/L α -LA for 60 minutes. (K) Total GLP-1 in the media from STC-1 cells treated with 50 μ mol/L α -LA for 60 minutes in the presence or absence of 0.5 μ mol/L GSK. (L) Western blot analysis in ileal scrapes of *Vhl^{ΔIE}* mice. n = 5–6 mice per group. (M) Western blot analysis in the ileal explants of *Vhl^{ΔIE}* mice treated with 50 μ mol/L α -LA for 60 minutes. Western blot for pERK in GSK-treated (N) C57BL/6, (O) *Vhl^{ΔIE}* mice. (P) Serum total GLP-1 in fasted *Vhl^{ΔIE}* mice orally gavaged with GSK at 3 mg/kg body weight. (Q) qPCR analysis for lipid-sensing genes in ileal scrapes of *Vhl^{ΔIE}* mice orally gavaged with GSK. All data are presented as means \pm SEM. * $P \leq .05$, ** $P \leq .01$, and *** $P \leq .001$ as analyzed by 2-tailed Student *t* test or 1-way analysis of variance with Tukey correction. DAPI, 4',6-diamidino-2-phenylindole; Veh, vehicle.

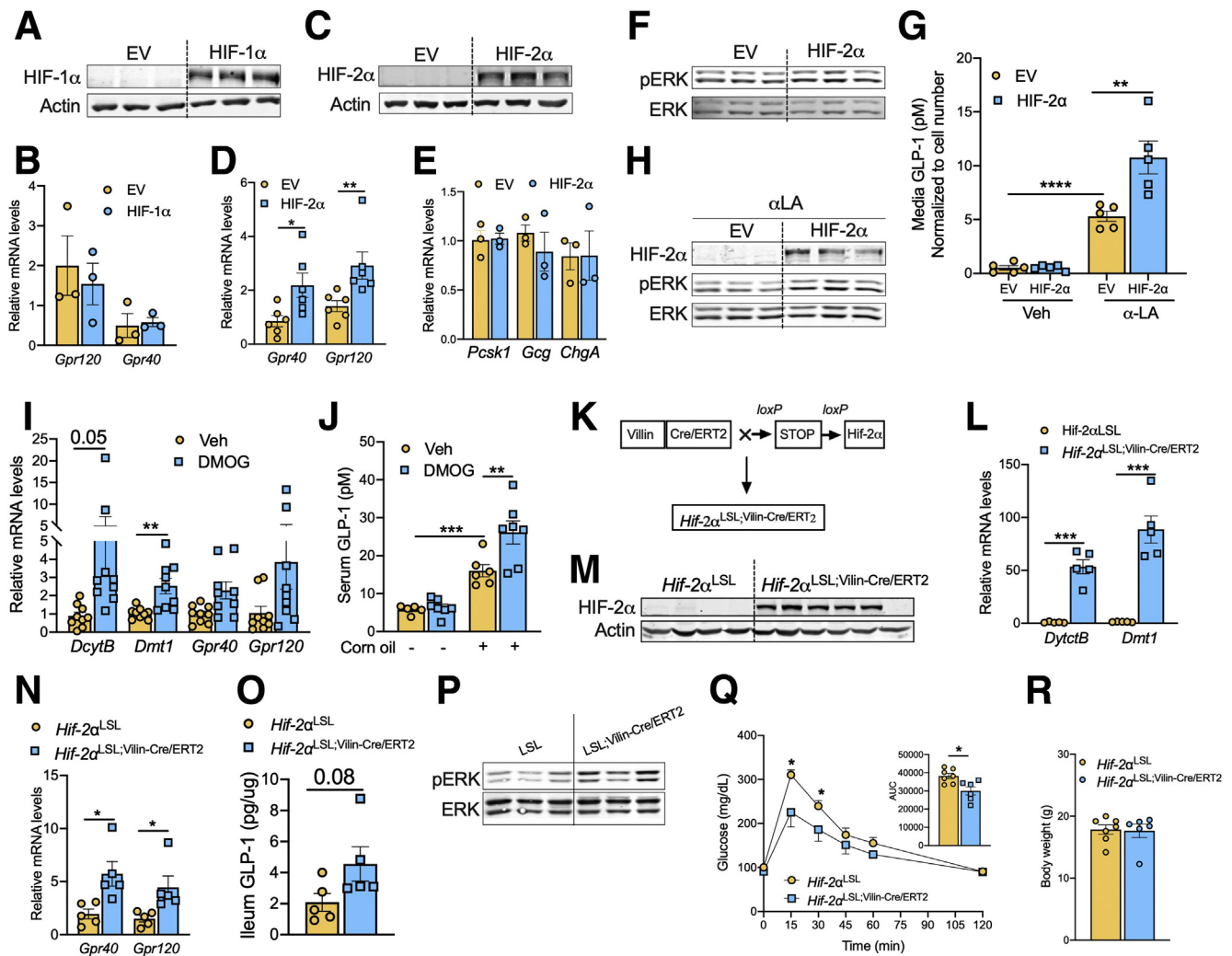


Figure 3. HIF-2 α promotes lipid sensing and GLP-1 secretion in L-cells. (A) Western blot analysis in STC-1 cells transiently overexpressing HIF-1 α for 48 hours. (B) qPCR analysis for lipid-sensing genes in STC-1 cells transiently overexpressing HIF-1 α for 48 hours. (C) Western blot analysis in STC-1 cells transiently overexpressing HIF-2 α for 48 hours. qPCR analysis for (D) lipid-sensing genes and (E) L-cell differentiation marker genes in STC-1 cells transiently overexpressing HIF-2 α for 48 hours. (F) Western blot analysis in STC-1 cells transiently overexpressing HIF-2 α for 48 hours. (G) Total GLP-1 measured in the media and (H) Western blot analysis in STC-1 cells transiently overexpressing HIF-2 α for 48 hours and treated with 50 μ mol/L α -LA for 60 minutes. (I) qPCR analysis for HIF target and lipid-sensing genes in the small intestine of male and female C57BL/6 mice injected intraperitoneally with DMOG at 10 mg/kg body weight. (J) Serum total GLP-1 in response to corn oil (20 mL/kg body weight) in C57BL/6 mice treated with DMOG. (K) Experimental schema showing generation of *Hif-2 α ^{LSL;VilIn-Cre/ERT2}* mice. (L) qPCR analysis for HIF-2 α target genes in small intestine of *Hif-2 α ^{LSL;VilIn-Cre/ERT2}* mice. (M) Western blot analysis in small intestine of *Hif-2 α ^{LSL;VilIn-Cre/ERT2}* mice. (N) qPCR analysis for lipid-sensing genes in the small intestines of *Hif-2 α ^{LSL;VilIn-Cre/ERT2}* mice. (O) Ileum GLP-1 levels and (P) Western blot analysis in small intestine of *Hif-2 α ^{LSL;VilIn-Cre/ERT2}* mice. (Q) IPGTT in chow-fed 6- to 7-week-old male *Hif-2 α ^{LSL;VilIn-Cre/ERT2}* mice. (R) Body weight of *Hif-2 α ^{LSL;VilIn-Cre/ERT2}* mice. All data are presented as means \pm SEM. * P \leq .05, ** P \leq .01, *** P \leq .001, and **** P \leq .0001 as analyzed by 2-tailed Student t test or 1-way analysis of variance with Tukey correction. AUC, area under curve; EV, empty vector; STOP, STOP; Veh, vehicle.

HIF-2 α Is an Essential Regulator of Intestinal Lipid Sensing and GLP-1 Secretion

Based on our data that intestinal HIF signaling is induced by fasting (Figure 1A and B), we assessed whether metabolic cues regulate lipid-sensing genes via HIF-2 α . qPCR analysis showed that fasting significantly increases the mRNA levels of *Gpr40* and *Gpr120* in the small intestines (Figure 6A). We show that acute inhibition of HIF-2 α using the HIF-2 α -specific inhibitor PT-2385 abolishes the fasting-

mediated induction of *Gpr40* and *Gpr120* mRNA (Figure 6B). Moreover, PT-2385-treated mice showed attenuated corn oil-stimulated GLP-1 secretion (Figure 6C). Together, our data suggest that intestinal HIF-2 α induced by fasting primes the intestine for optimal lipid-mediated GLP-1 secretion.

To further elucidate the essential role of HIF-2 α in lipid sensing, we assessed mice with intestinal epithelial-specific knockout of HIF-2 α (*Hif-2 α ^{ΔIE}*). As expected, *Gpr120* and

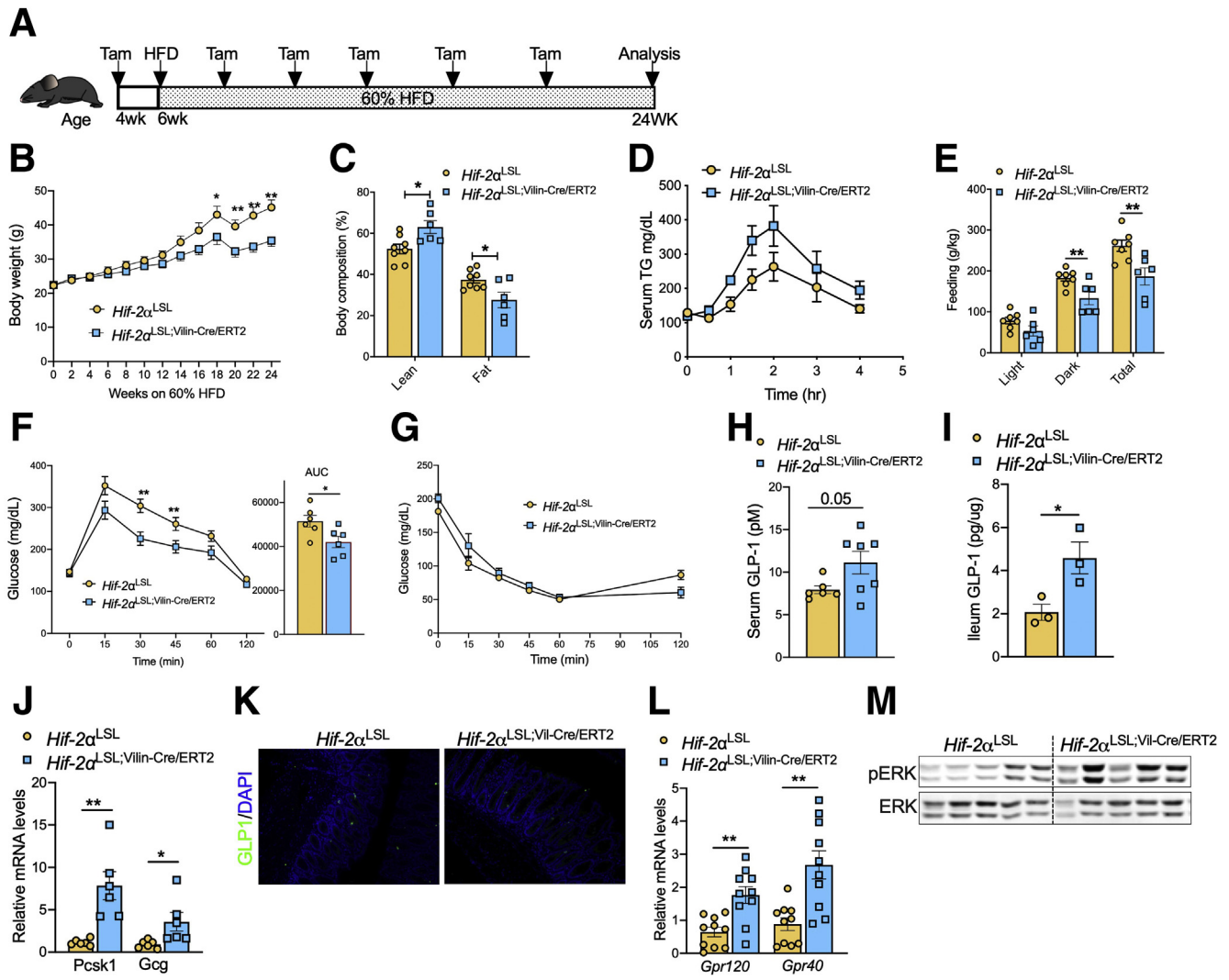
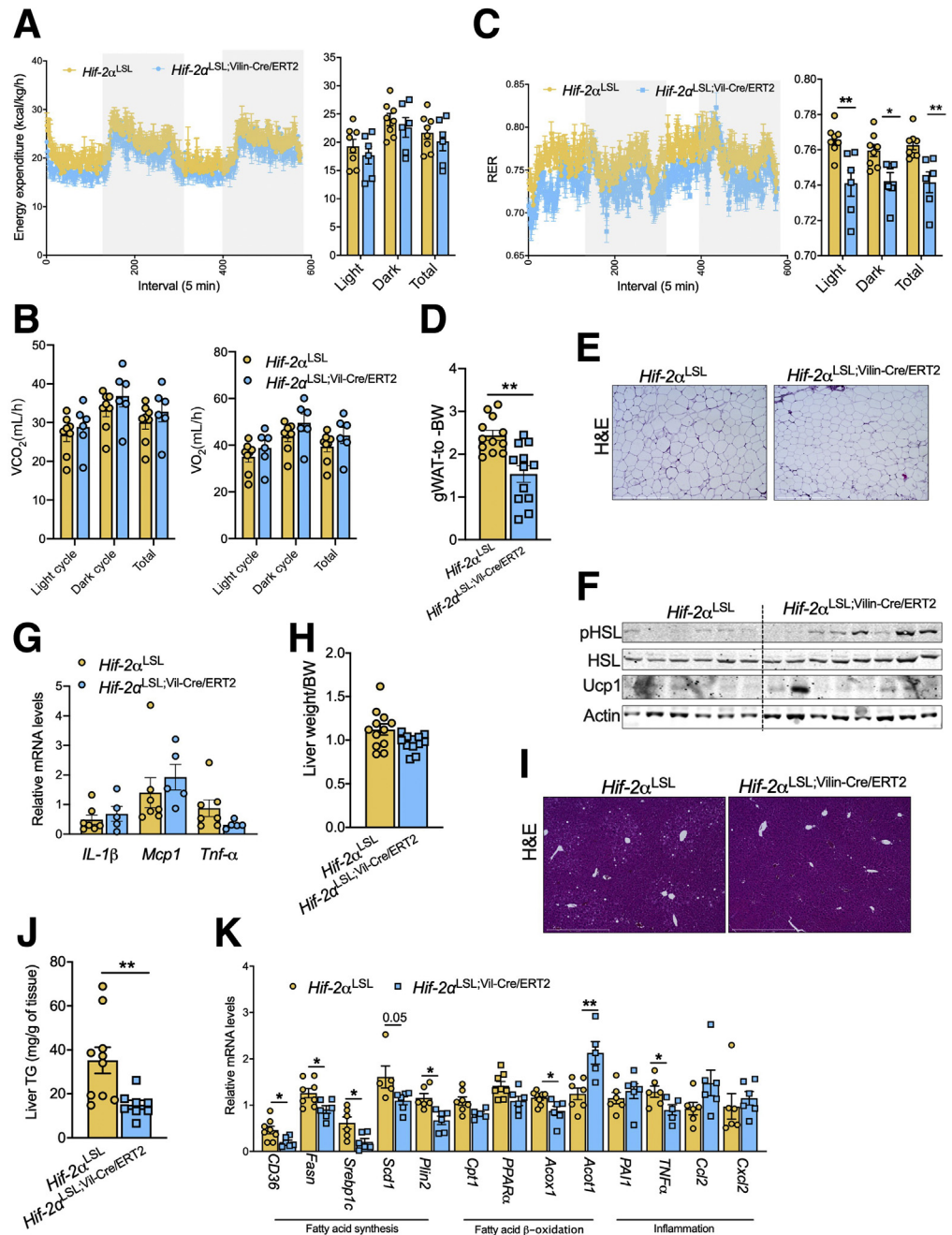


Figure 4. Intestinal HIF-2 α improves diet-induced glucose tolerance. (A) Experimental schema. (B) Body weight (in grams) for the indicated time points during 60% HFD feeding. (C) Lean and fat mass of HFD-fed *Hif-2 α ^{LSL};Vil1-Cre/ERT2* mice. (D) Serum triglycerides during the lipid tolerance test. (E) Three-day cumulative food intake. (F and G) Blood glucose excursion, area under curve (AUC) during intraperitoneal glucose tolerance test (ipGTT) and insulin tolerance test (ITT) in HFD-fed *Hif-2 α ^{LSL};Vil1-Cre/ERT2* mice. (H) Serum and (I) ileum total GLP-1 levels. (J) qPCR analysis for glucagon processing genes in the small intestine of HFD-fed *Hif-2 α ^{LSL};Vil1-Cre/ERT2* mice. (K) Immunostaining for GLP-1 in small intestine. Magnification: 20 \times . (L) qPCR analysis for lipid-sensing genes in the small intestine of HFD-fed *Hif-2 α ^{LSL};Vil1-Cre/ERT2* mice. (M) Western blot analysis in small intestine of HFD-fed *Hif-2 α ^{LSL};Vil1-Cre/ERT2* mice. All data are presented as means \pm SEM. * $P \leq .05$ and ** $P \leq .01$ as analyzed by 2-tailed Student *t* test. DAPI, 4',6-diamidino-2-phenylindole; Tam, tamoxifen; TG, triglyceride.

Gpr40 mRNA levels were reduced significantly in the small intestines of fasted *Hif-2 α ^{ΔIE}* mice (Figure 6D); however, no difference was noted under the fed condition (Figure 6E). Moreover, meal-stimulated GLP-1 secretion was attenuated significantly in *Hif-2 α ^{ΔIE}* mice (Figure 6F), suggesting that HIF-2 α signaling is an essential regulator of postprandial GLP-1 secretion. DMOG treatment induces both HIF-1 α and HIF-2 α , we therefore evaluated the specificity of the HIF isoform involved in DMOG-mediated potentiation of GLP-1 secretion. To this end, we treated *Hif-2 α ^{ΔIE}* mice with or without DMOG to assess corn oil-stimulated GLP-1 secretion. Our data show that DMOG failed to potentiate GLP-1 secretion in *Hif-2 α ^{ΔIE}* mice (Figure 6G), indicating that DMOG promotes GLP-1 secretion via HIF-2 α .

We previously reported that disruption of intestinal HIF-2 α did not result in any difference in body weight or glucose homeostasis when fed on a chow diet.²⁶ Consistently, body weight, glucose tolerance, and insulin tolerance were similar between 8-week-old *Hif-2 α ^{F/F}* and *Hif-2 α ^{ΔIE}* mice maintained on a chow diet (Figure 6H–J). However, *Hif-2 α ^{ΔIE}* mice develop mild but significant glucose intolerance and insulin resistance at 13 months, albeit with no difference in body weight (Figure 6K–M). qPCR analysis in the small intestine showed an age-dependent increase in the mRNA levels of *Hif-2 α* , *Gpr120*, and *Gpr40* (Figure 6N), which was abolished in *Hif-2 α ^{ΔIE}* mice. Further analysis showed significantly lower levels of serum GLP-1 in *Hif-2 α ^{ΔIE}* mice

Figure 5. Intestinal HIF-2 α protects against diet-induced obesity and hepatic steatosis. (A) Energy expenditure, (B) V_{CO_2} and V_{O_2} , and (C) respiratory energy ratio (RER) (normalized to lean body mass) assessed by indirect calorimetry in HFD-fed *Hif-2 α ^{LSL;Vil-in-Cre/ERT2}* mice. (D) Gonadal white adipose tissue weight normalized to body weight and (E) H&E in gonadal white adipose tissue showing smaller adipocytes in HFD-fed *Hif-2 α ^{LSL;Vil-in-Cre/ERT2}* mice. Magnification: 10 \times . (F) Western blot for the indicated proteins in gonadal white adipose tissue. $n = 7-8$ mice per group. (G) qPCR analysis for inflammatory markers in the gonadal white adipose tissue. (H) Liver weight and (I) liver H&E analysis. Magnification: 10 \times . (J) Liver triglyceride levels normalized to tissue weight. (K) qPCR analysis in the livers of HFD-fed *Hif-2 α ^{LSL;Vil-in-Cre/ERT2}* mice. All data are presented as means \pm SEM. * $P \leq .05$ and ** $P \leq .01$ as analyzed by 2-tailed Student t test. BW, body weight; gWAT, gonadal white adipose tissue; HSL, hormone sensitive lipase; pHSL, phospho hormone sensitive lipase; TG, triglyceride; Ucp1, uncoupling protein 1.



(Figure 6O). Collectively, our data suggest that intestinal HIF-2 α is essential for the intestinal expression of lipid-sensing genes and GLP-1 levels, and disruption of intestinal HIF-2 α leads to age-associated metabolic derangements.

Discussion

For decades, it has been known that microvascular circulation decreases during fasting, contributing to low oxygen levels in the intestinal epithelia.^{15,16,38-41} Several studies have shown that the degree of hypoxia determines

the tissue/cell response. For example, subtle and/or rapid changes in oxygen tension lead to a HIF response that promotes physiological adaptation to increase intestinal iron absorption via HIF-2 α ⁴² or promotes barrier function via HIF-1 α .^{19,43} However, chronic and robust HIF-2 α activation integrates with inflammatory cues to induce colitis.⁴⁴ Here, using a genetic model mimicking hypoxic induction, we show that intestinal HIF signaling improves glucose homeostasis, glucose-stimulated insulin secretion, and increases steady-state GLP-1 levels. Oral but not parenteral administration of nutrients is necessary to observe the glucoregulatory effects of GLP-1.⁴⁵ However,

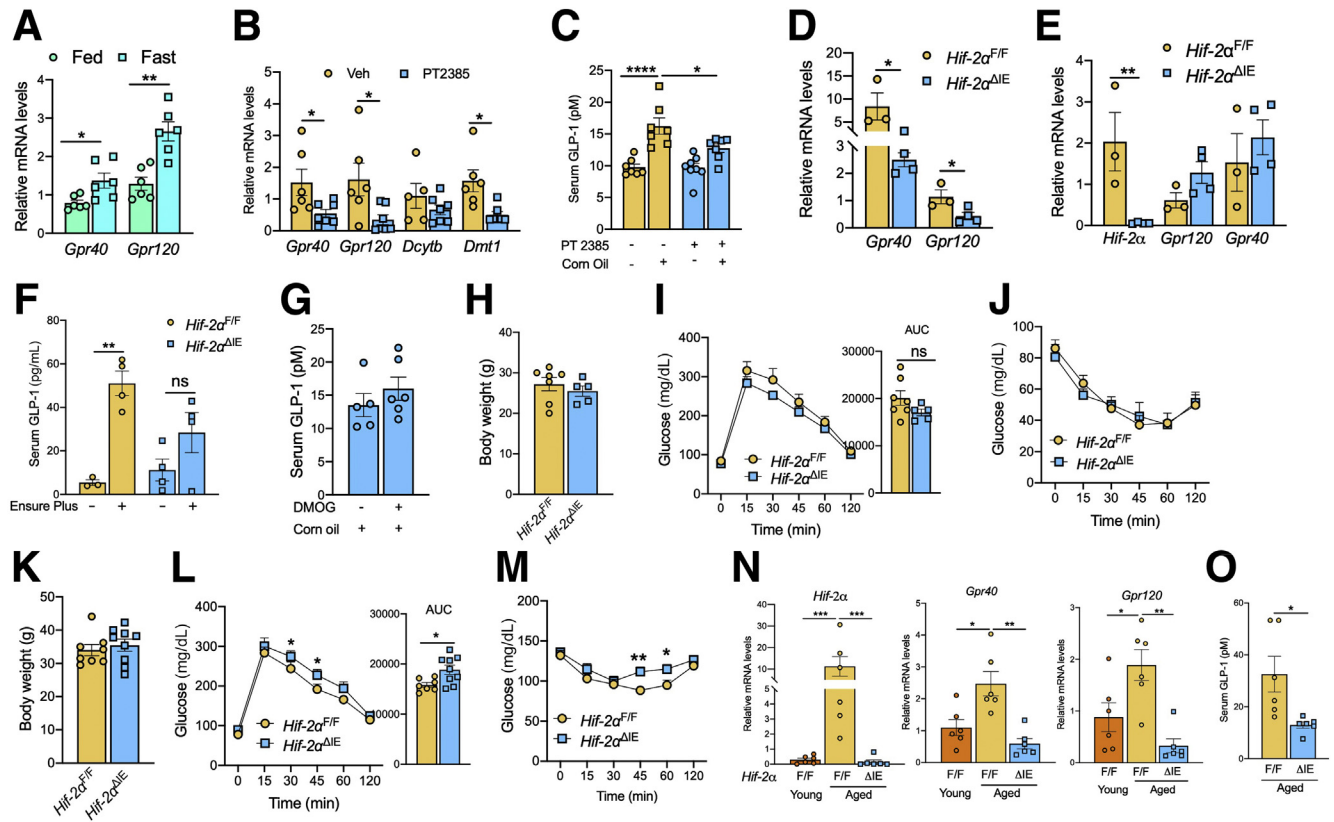


Figure 6. HIF-2 α is essential for fasting and regulates aging-mediated lipid sensing and GLP-1 secretion. (A) qPCR analysis in the small intestine of fed and 16-hour fasted C57BL/6 mice. (B) qPCR analysis in the small intestine of 6- to 8-week-old male and female C57BL/6 mice under 16-hour fasted conditions with or without PT-2385 (MedChem Express, Manmout Junction, NJ) at 50 mg/kg body weight. (C) Corn oil-induced GLP-1 (total) in fasted C57BL/6 mice treated with or without PT-2385 (50 mg/kg BW). (D) qPCR analysis in the small intestine of fasted *Hif-2 $\alpha^{\Delta IE}$* mice. (E) qPCR analysis in the small intestine of fed *Hif-2 $\alpha^{\Delta IE}$* mice. (F) Serum total GLP-1 levels in *Hif-2 $\alpha^{\Delta IE}$* mice challenged with mixed-meal (Ensure Plus at 2 g/kg body weight). (G) Corn oil-induced total GLP-1 in fasted *Hif-2 $\alpha^{\Delta IE}$* mice treated with or without DMOG (10 mg/kg BW). (H) Body weight of 6- to 8-week-old *Hif-2 $\alpha^{\Delta IE}$* mice. (I) Blood glucose excursion and area under curve (AUC) during intraperitoneal glucose tolerance test (ipGTT) and (J) intraperitoneal insulin tolerance test (ipITT) in 6- to 8-week-old *Hif-2 $\alpha^{\Delta IE}$* mice. (K) Body weight of 13-month-old *Hif-2 $\alpha^{\Delta IE}$* mice. (L) Blood glucose excursion and AUC during ipGTT and (M) ipITT in 13-month-old *Hif-2 $\alpha^{\Delta IE}$* mice. (N) qPCR analysis for the indicated genes in the small intestinal scrapes of young and old *Hif-2 $\alpha^{F/F}$* and *Hif-2 $\alpha^{\Delta IE}$* mice. (O) Serum total GLP-1 levels in 13-month-old *Hif-2 $\alpha^{\Delta IE}$* mice. All data are presented as means \pm SEM. * $P \leq .05$, ** $P \leq .01$, *** $P \leq .001$ and **** $P \leq .0001$ as analyzed by 2-tailed Student *t* test or 1-way analysis of variance with Tukey correction.

Vhl^{ΔIE} mice had lower glucose excursion in response to IP glucose challenge, which is abolished by exendin 9-39. Thus, we attribute the basal increase in GLP-1 to HIF-mediated improvement in glucose homeostasis.

Intestinal release of GLP-1 could be induced by increasing L-cell content or augmenting GLP-1 secretion.^{4,46} We found that intestinal HIF potentiated GLP-1 secretion in response to lipids (LCFA), consistent with the increased intestinal expression of the lipid sensors GPR40 and GPR120. Ligand-mediated activation of GPR40 and GPR120 have redundant functions in GLP-1 secretion.^{6,8} Our data that inhibition of GPR40 is sufficient to abrogate the HIF-mediated increase in GLP-1 indicates that intestinal HIF promotes GLP-1 predominantly through GPR40. Furthermore, we identified ERK as the downstream mediator of HIF-GPR40 regulation of GLP-1. Thus, we propose a novel mechanism in which hypoxia signaling regulates metabolic homeostasis via GPR40-mediated lipid sensing and GLP-1 secretion.

Our data show that HIF-2 α but not HIF-1 α induces GPR40 in L-cells. This observation is consistent with the differential role of HIF-1 α and HIF-2 α in regulating distinct sets of genes.^{47,48} HIF-2 α expression did not affect the basal GLP-1 levels in L-cells, but potentiated the ligand-stimulated GLP-1 secretion. However, HIF-2 α activation increased both basal and ligand-mediated GLP-1 secretion in vivo. Given that intestinal L-cells are exposed to luminal fatty acids,⁴⁹ we attribute the increased basal GLP-1 levels to sensing of luminal lipids via GPR40.

Activation of intestinal HIF-2 α attenuated diet-induced weight gain, glucose intolerance, and hepatic steatosis. These metabolic effects are associated with canonical GLP-1 functions such as decreased food intake, hepatic lipogenesis, and increased adipose tissue lipolysis. Thus, the metabolic effects in HIF-2 α -activated mice could be attributed to increased GPR40-GLP-1 signaling and suggest intestinal HIF-2 α prevents diet-induced

metabolic perturbations. However, this observation contradicts our recent report that disruption of intestinal HIF-2 α protects against diet-induced glucose intolerance and hepatic steatosis owing to a decrease in intestinal ceramide synthesis.²⁶ Accumulating evidence supports the view that an obesity-associated increase in GLP-1 counteracts diet-induced glucose intolerance and hepatic steatosis via multiple mechanisms.^{50,51} We postulate that the paradox in our findings could be attributed to increased GLP-1 levels in HIF-2 α -overexpressing mice. Thus, our study highlights the complex role of intestinal HIF-2 α in metabolic homeostasis, depending on the cell type of its activation. Whether GLP-1 released from L-cells counteracts ceramide synthesis in enterocytes via a paracrine effect needs further investigation.

Our study also provides empiric evidence that HIF-2 α regulation of lipid sensing and GLP-1 is a physiologically relevant mechanism essential for postprandial GLP-1 secretion. We show that acute pharmacologic inhibition of HIF-2 α attenuates fasting-mediated GPR40/120 expression, suggesting that HIF-2 α primes the lipid-sensing mechanism to respond swiftly to dietary lipids. This concept is supported further by our observation that pharmacologic inhibition of HIF-2 α abolishes postprandial GLP-1 secretion stimulated by lipids. We show that disruption of HIF-2 α in the intestine reduces GPR40/120 expression and meal-stimulated GLP-1 secretion. Furthermore, a DMOG-mediated increase in GLP-1 is dependent on intact intestinal HIF-2 α signaling. Despite an impairment in GLP-1 secretion, disruption of HIF-2 α does not lead to any metabolic phenotype in young mice, consistent with our previous report.²⁶ Remarkably, older intestine-specific HIF-2 α knockout mice developed glucose and insulin intolerance, associated with decreased GPR40 and GLP-1 levels. Thus, we postulate that intestinal HIF-2 α is crucial to protect against age-associated metabolic ailments, potentially via GLP-1 signaling.

Conclusions

Compelling evidence shows that GLP-1-based therapies are superior in restoring normoglycemia in type 2 diabetic patients.^{52–54} However, no current treatments leverage the endogenous GLP-1 owing to an incomplete understanding of the GLP-1 secretory mechanisms. Our data provide a strong mechanistic insight into the role of HIF-2 α in regulating GLP-1 secretion through lipid sensing. Given that DMOG potentiates GLP-1 secretion via intestinal HIF-2 α and targeted delivery of PHD inhibitors to the intestine is feasible,^{55,56} our study provides a strong rationale for future investigations determining the pharmacologic targeting of intestinal HIF signaling in metabolic diseases. Further investigations using mouse models with L-cell specific HIF-2 α gain- or loss-of-function studies also may unfold novel targets to stimulate endogenous GLP-1 production.

Limitations

The intestinal-epithelial VHL knockout mice and DMOG treatment assessed in this study induce both HIF-1 α and

HIF-2 α . VHL also is known to elicit HIF-independent functions that could affect metabolic homeostasis. Furthermore, the villin Cre-mediated recombination induces HIF-2 α in all intestinal epithelial cells. Therefore, studies with L-cell-specific HIF-2 α gain- or loss-of-function will unravel novel targets to induce endogenous GLP-1 production.

Methods

Animals

Mice were housed up to 4 (males) or 5 per cage (females), kept under a 12-hour light/dark cycle, and maintained on respective regular chow (D12450J; Research Diets, New Brunswick, NJ), or HFD (60% kcal from fat, D12492; Research Diets). All mice were given free access to food and water. All experiments were performed using age- and sex-matched littermates, unless indicated in the figure legends. The generation and use of hypoxia reporter mice (ODD domain-luc), *Vhl* ^{Δ IE}, *Hif-2 α* ^{Δ IE}, and *Hif-2 α* ^{LSL;Villin-Cre/ERT2} were described previously.^{26,57} Littermate controls that do not express Cre recombinase were used as controls for all studies. The intestinal expression of HIF-2 α was temporally induced in *Hif-2 α* ^{LSL;Villin-Cre/ERT2} mice by IP injection of tamoxifen (20 mg/kg body weight) dissolved in corn oil. Littermate controls (*Hif-2 α* ^{LSL}) mice also were injected with tamoxifen. For HFD studies, *Hif-2 α* ^{LSL} and *Hif-2 α* ^{LSL;Villin-Cre/ERT2} mice were injected with tamoxifen and then started on 60% HFD. Tamoxifen was administered to the mice once a month during HFD feeding. For IVIS imaging (Caliper Life Sciences, Hopkinton, MA), ODD-Luc were fasted overnight and then injected with D-luciferin at 50 mg/kg body weight, and after 15 minutes the small intestine was excised and imaged using the IVIS 200 imaging system. All animal experiments were approved by the Animal Care and Use Committee at the University of Michigan and the University of Pittsburgh.

In Vivo GLP-1 Secretion Studies

For corn oil-stimulated GLP-1 secretion, *Vhl*^{F/F} and *Vhl* ^{Δ IE} mice were fasted for 16 hours and challenged with a bolus of 20 mL/kg corn oil (Sigma-Aldrich, St. Louis, MO) administered by oral gavage. The blood was collected from the tail at 0 and 30 minutes after gavage. For MEK-ERK inhibition, GSK1120212 (Cayman Chemicals, Ann Arbor, MI) dissolved in dimethyl sulfoxide and diluted in phosphate-buffered saline (PBS) was administered by oral gavage at 3 mg/kg body weight and then mice were fasted immediately for 16 hours. Two hours before blood collection, another dose of GSK1120212 was provided. For GPR40 antagonism, GW1100 (Cayman Chemicals) dissolved in dimethyl sulfoxide and diluted in PBS were administered by oral gavage at 2.5 mg/kg body weight. Two hours before blood collection, mice again were administered with another dose of GW1100. For HIF-2 α inhibitor studies, mice were treated with PT-2385 (MedChemExpress, Monmouth Junction, NJ) at 50 mg/kg body weight dissolved in 10% EtOH+30% polyethylene glycol 400 (PEG400)+60% microcrystalline tyrosine or vehicle alone and fasted immediately. For HIF activation studies, mice were treated with DMOG (MedChemExpress) at 10 mg/kg body

weight dissolved in dimethyl sulfoxide (further diluted in PBS) or vehicle. Two hours before blood collection, mice were administered another dose of DMOG. For mixed-meal-induced GLP-1 secretion, mice were fasted overnight for 16 hours and challenged with a bolus of 2 g/kg glucose in Ensure Plus (Abbott Laboratories, Columbus, OH), administered by oral gavage. The blood was collected from the tail at 0 and 15 minutes after gavage. For all the assays measuring GLP-1, blood was collected in the tubes containing dipeptidyl peptidase IV (DPP-IV) inhibitor Diprotein A (100 $\mu\text{mol/L}$), and serum was separated by centrifugation at 7500g for 10 minutes at 4°C.

Cell Culture, Transfection, and GLP-1 Secretion Assays

STC-1 cells (mouse intestinal neuroendocrine cells; ATCC, Manassas, VA) were cultured in Dulbecco's modified Eagle medium (DMEM) containing 10% fetal bovine serum. Cells were maintained at 37°C and 5% CO₂. For transient expression studies, STC-1 cells at 60%–70% confluence were transfected with 5 μg empty vector or plasmids encoding HIF-1 α complementary DNA (cDNA) or HIF-2 α cDNA using Lipofectamine 3000 transfection reagent (ThermoFisher Scientific Waltham, MA). The cells were analyzed 48 hours after transfection. For the GLP-1 secretion assay, an equal number of cells were plated in 6-well plates and transfected with an empty vector or HIF-2 α . After 48 hours, the cells were washed twice with Hanks balanced salt solution (ThermoFisher Scientific) and treated with α -linolenic acid (50 $\mu\text{mol/L}$) in DMEM for 60 minutes at 37°C in the presence of Diprotein A (100 $\mu\text{mol/L}$; Cayman Chemicals). For GLP-1 secretion with MEK inhibitor, cells were treated with α -linolenic acid (50 $\mu\text{mol/L}$) in the presence or absence of GSK1120212 (Cayman Chemicals) at 0.5 $\mu\text{mol/L}$ and incubated for 60 minutes at 37°C. Total GLP-1 was measured in the media using an enzyme-linked immunosorbent assay kit (Crystal Chem, IL).

RNA Isolation and Real-Time Reverse-Transcription PCR

Total RNA was extracted from the small intestine (ileum), liver, and adipose tissue using TRIzol reagent (ThermoFisher Scientific) as per standard protocol. cDNA was prepared with 1 μg total RNA using Moloney murine leukemia virus (Mu-MLV) reverse transcriptase (Promega, Madison, WI). The relative expression of genes was assessed with SYBR Green master mix (Radiant Molecular Tools, Fort Lauderdale, FL) using QuantStudio 3 Station qPCR machine (Applied Biosystems, Foster City, CA). The relative expression of target genes was calculated using a comparative delta threshold cycles (ΔCT) method after normalizing to β -actin. The primer sequences used were as follows: *Ffar1* forward: 5'-AGGCGCTCTCCTCACACTC-3', reverse: 5'-CTAGCCACATTGGAGGCATT-3'; *Ffar4* forward: 5'-CCATCCCTTAGTGCTCGTC-3', reverse: 5'-TGCGGAA-GAGTCGGTAGTCT-3'; *Gpr142* forward: 5'-TGCTGCCTA-CAGTCAATGGT-3', reverse: 5'-TGACGATATCTGAAGCCGTG-3'; *Glut1* forward: 5'-CAAGTCTGCATTGCCCATGAT-3',

reverse: 5'-CAAGTCTGCATTGCCCATGAT-3'; β -actin forward: 5'-TATTGGCAACGAGCGTTCC-3', reverse: 5'-GGCA-TAGAGGTCTTTACGGATGT-3'; *Hif-1 α* forward: 5'-GGGTACAAGAAACCACCCAT-3', reverse: 5'-GAGGCTGTGTC-GACTGAGAA-3'; *Hif-2 α* forward: 5'-AGTTCCTTCGGACACA-TAAG-3', reverse: 5'-GCTTTCAGGTACAAGTTATCCATTT-3'; *DcytB* forward: 5'-CATCCTCGCCATCATCTC-3', reverse: 5'-GGCATTGCCTCCATTTAGCTG-3'; *Dmt1* forward: 5'-TGTTTGATTGCATTGGGTCTG-3', reverse: 5'-CGCTCAGCAG-GACTTTCGAG-3'; *Pgk1* forward: 5'-CAAATTTGATGA-GAATGCCAAGACT-3', reverse: 5'-TTCTTGCTGCTCTCAGTACCAC-3'; *Gcg* forward: 5'-GCTTA-TAATGCTGGTGCAAG-3', reverse: 5'-TTCATCTCAT-CAGGGTCTC-3'; *Ngn3* forward: 5'-GCATGCACAACCTCAACTC-3', reverse: 5'-TTTGTAAGTTTGGCGTCATC-3'; *ChgA* forward: 5'-GCAGGC-TACAAAGCGATCCA-3', reverse: 5'-CTCTGTCTTTCCATCTC-CATCCA-3'; *Pcsk1* forward: 5'-TCTGGTTGTCTGGACCTCTGAGT-3', reverse: 5'-CAT-CAAGCCTGCCCATTTCTTT-3'; *Cd36* forward: 5'-CCTGCAAATGTCAGAGGAAA-3', reverse: 5'-GCGA-CATGATTAATGGCACA-3'; *Srebp1* forward: 5'-TGTTGTGATGAGCTGGAG-3', reverse: 5'-GGCTCTGGAACA-GACACTGG-3'; *Cpt1a* forward: 5'-CCAGGTACAGTGGGA-CATT-3', reverse: 5'-GAACTTGCCCATGTCCTTGT-3'; *Acox1* forward: 5'-TCGAAGCCAGCGTTACGAG-3', reverse: 5'-ATCTCCGTCTGGGCGTAGG-3'; *Fasn* forward: 5'-GTTGGCCAGAACTCCTGTA-3', reverse: 5'-GTCGTCTGCCTCCAGAGC-3'; *Pai1* forward: 5'-ACGCTGGTGCTGGTGAATGC-3', reverse: 5'-ACGGTGCTGC-CATCAGACTTGTG-3'; *Tnfa* forward: 5'-AGGGTCTGGGCCA-TAGAACT-3', reverse: 5'-CCACCACGCTCTTCTGTCTAC-3'; *Ccl2* forward: 5'-CTCACCTGTGCTACTCATTC-3', reverse: 5'-ACTACAGTCTTTGGGACAC-3'; *Acot1* forward: 5'-ATGG-CAGCAGCTCCAGACT-3', reverse: 5'-ATCTCCGTCTGGGCG-TAGG-3'; *Ppara* forward: 5'-AGAGCCCCATCTGTCTCTC-3', reverse: 5'-ACTGGTAGTCTGCAAAACCAA-3'; *Plin2* forward: 5'-CTCAGGAGGAGCTGGAGATG-3', reverse: 5'-TCAAT-CAGGTGGACAGTGA-3'; *Scd1* forward: 5'-CAGCC-GAGCCTTGAAGTTC-3', reverse: 5'-GCTCTACACTGCCTCTTCG-3'; *Cxcl1* forward: 5'-CTGCACC-CAAACCGAAGTC-3', reverse: 5'-AGCTTCAGGGTCAAGG-CAAG-3'; *Il1 β* forward: 5'-AAGAGCTTCAGGCAGGCAGTATCA-3', reverse: 5'-TGCAGCTGTCTAGGAACGTCA-3'; *Mcp1* forward: 5'-AGCTCTCTTCTCCTCCACCA-3', reverse: 5'-GGCGTTAACTGCATCTGGCT-3'.

Western Blot

Total protein lysates for immunoblotting were prepared using radioimmunoprecipitation assay lysis buffer (0.5% NP-40, 0.1% sodium deoxycholate, 150 mmol/L NaCl, 50 mmol/L Tris-Cl, pH 7.5) containing 1 mmol/L phenylmethylsulphonyl fluoride, protease inhibitor cocktail (Sigma-Aldrich) and 2 mmol/L sodium orthovanadate. Protein concentration was determined using a protein assay kit (Bio-Rad, Hercules, CA), and proteins were resolved on a 9% polyacrylamide gel and transferred onto nitrocellulose or polyvinylidene difluoride membranes (Bio-Rad).

Nonspecific binding was blocked using 3% skim milk, and membranes were incubated overnight at 4°C with primary antibodies such as ERK, pERK (Cell Signaling Technology, Denver, MA), HIF-2 α (Novus Biologicals, Littleton, CO), and HIF-1 α (Abcam, Waltham, MA). Secondary antibodies conjugated with DyLight (Cell Signaling Technology) were added to the membranes and visualized using the Odyssey CLx Imaging System (LI-COR, Lincoln, NE).

Liver Triglyceride Assay

Liver triglycerides were quantified as described previously.⁵⁸ Briefly, liver tissue was homogenized in chloroform:methanol (2:1) and incubated for 60 minutes at room temperature on a shaker, followed by acidification with 1 mol/L H₂SO₄. The organic phase containing the lipids was collected by centrifugation at 2000g for 10 minutes. The triglycerides from the organic phase and serum were measured using colorimetric Infinity Triglyceride Reagent (ThermoFisher Scientific). Tissue triglyceride levels were normalized to their respective weights.

Ileal Explant Ex Vivo Studies

The ileum from *Vhl*^{F/F} and *Vhl* ^{Δ 1E} was excised and washed thoroughly in glucose-free Krebs-Ringer bicarbonate buffer (138 mmol/L NaCl, 5.6 mmol/L KCl, 2.6 mmol/L CaCl₂, 1.2 mmol/L MgCl₂, 4.2 mmol/L NaHCO₃, 1.2 mmol/L NaH₂PO₄, and 10 mmol/L HEPES; pH 7.4) and cut into small pieces. The ileal explants were weighed, transferred to DMEM/F12, and treated with α -linolenic acid (50 μ mol/L) for 60 minutes at 37°C. The whole-cell extract for Western analysis was prepared using radioimmunoprecipitation assay buffer.

Tissue Histology and Immunofluorescence

Liver and white adipose tissue were fixed in 10% PBS-buffered formalin (ThermoFisher Scientific), embedded in paraffin, and 6 micron sections were prepared. H&E staining was performed using the standard protocol. For immunofluorescence, antigen retrieval was performed using citrate buffer (pH 6), and the sections were blocked in 10% goat serum in phosphate buffered saline Tween-20 (PBST) for 30 minutes at room temperature. Sections were incubated in primary antibody (GLP-1) overnight, followed by multiple washing with PBS. Sections then were probed with secondary antibody conjugated with Alexa Flour (Cell Signaling), and images were captured using a Nikon microscope (Nikon Instruments Inc. Melville, NY). The number of L-cells was counted manually.

Body Composition and Indirect Calorimetry

Body fat and lean mass of conscious mice were determined by EchoMRI (EchoMRI, LLC, Houston, TX). The whole-body composition as a percentage of fat and lean mass were calculated for individual mice by dividing the tissue mass by body weight. Energy homeostasis was measured by indirect calorimetry using the Promethion Multiplexed Metabolic Cage System (Sable Systems, Las Vegas, NV).⁵⁹ Mice were housed in individual chambers with

free access to food and water. The first 24 hours were considered an acclimatization period, and mice were studied for 72 hours. Energy expenditure was normalized to lean body mass.

Metabolic Tests

For intraperitoneal glucose tolerance test (ipGTT), dextrose was injected at 1.5 g/kg body weight in overnight fasted mice. For intraperitoneal insulin tolerance test (ipITT), insulin (Eli Lilly, Indianapolis, IN) was injected at 0.75 U/kg body weight in mice fasted for 6 hours. Glucose was measured from the tail vein blood at 0, 15, 30, 45, 60, and 120 minutes using a glucometer (Bayer, Parsippany, NJ). The area under the curve over 120 minutes was calculated using a standard formula. For GLP-1-receptor agonists, mice were injected intraperitoneally with either vehicle (PBS) or exendin 9-39 (Cayman Chemicals) 1 hour before glucose administration. For acute-phase, glucose-stimulated insulin secretion, mice were anesthetized with avertin, and then glucose was administered intraperitoneally at 2 g/kg body weight and blood was collected by retro-orbital bleeding. For the lipid tolerance test, corn oil (200 μ L/mice) was gavaged to the mice, and serum was collected at the indicated time points.

Tissue, Media, and Serum GLP-1 Assay

Small intestinal and pancreatic tissue was homogenized in 200 μ L lysis buffer (50 mmol/L Tris HCl [pH 8 at 4°C], 1 mmol/L EDTA, 10% glycerol [wt/vol], 0.02% Tween-20) supplemented with protease inhibitors and 100 μ mol/L of Diprotein A. Total GLP-1 (Crystal Chem, Elk Grove Village, IL and Meso Scale Discovery Rockville, MD) was measured in the tissue supernatant, media, and serum following the manufacturer's recommendation. Tissue GLP-1 levels were normalized to protein content.

Statistical Analysis

All the data are represented as means \pm SEM. Statistical analysis was performed using GraphPad Prism; version 8.1.2. (San Diego, CA). The statistical difference between the 2 groups was determined by using a 2-tailed Student *t* test. To compare more than 2 groups, 1-way analysis of variance followed by the Tukey multiple-comparisons test was applied. The differences between groups were considered statistically significant at $P \leq .05$, and *P* values were calculated with a 95% CI. *P* values for the figures are indicated in the corresponding figure legends. All in vitro experiments were performed at least 2 times.

Data Access

All authors had access to all data and reviewed and approved the final manuscript.

References

1. Sun EWL, Martin AM, Young RL, Keating DJ. The regulation of peripheral metabolism by gut-derived hormones. *Front Endocrinol (Lausanne)* 2018;9:754.

2. Krieger JP. Intestinal glucagon-like peptide-1 effects on food intake: physiological relevance and emerging mechanisms. *Peptides* 2020;131:170342.
3. Shah M, Vella A. Effects of GLP-1 on appetite and weight. *Rev Endocr Metab Disord* 2014;15:181–187.
4. Muller TD, Finan B, Bloom SR, D'Alessio D, Drucker DJ, Flatt PR, Fritsche A, Gribble F, Grill HJ, Habener JF, Holst JJ, Langhans W, Meier JJ, Nauck MA, Perez-Tilve D, Pocai A, Reimann F, Sandoval DA, Schwartz TW, Seeley RJ, Stemmer K, Tang-Christensen M, Woods SC, DiMarchi RD, Tschop MH. Glucagon-like peptide 1 (GLP-1). *Mol Metab* 2019;30:72–130.
5. Reimann F, Habib AM, Tolhurst G, Parker HE, Rogers GJ, Gribble FM. Glucose sensing in L cells: a primary cell study. *Cell Metab* 2008;8:532–539.
6. Duca FA, Waise TMZ, Pepler WT, Lam TKT. The metabolic impact of small intestinal nutrient sensing. *Nat Commun* 2021;12:903.
7. Hirasawa A, Tsumaya K, Awaji T, Katsuma S, Adachi T, Yamada M, Sugimoto Y, Miyazaki S, Tsujimoto G. Free fatty acids regulate gut incretin glucagon-like peptide-1 secretion through GPR120. *Nat Med* 2005;11:90–94.
8. Ghislain J, Poitout V. Targeting lipid GPCRs to treat type 2 diabetes mellitus - progress and challenges. *Nat Rev Endocrinol* 2021;17:162–175.
9. Syed I, Lee J, Moraes-Vieira PM, Donaldson CJ, Sontheimer A, Aryal P, Wellenstein K, Kolar MJ, Nelson AT, Siegel D, Mokrosinski J, Farooqi IS, Zhao JJ, Yore MM, Peroni OD, Saghatelian A, Kahn BB. Palmitic acid hydroxystearic acids activate GPR40, which is involved in their beneficial effects on glucose homeostasis. *Cell Metab* 2018;27:419–427 e4.
10. Paschoal VA, Walenta E, Talukdar S, Pessentheiner AR, Osborn O, Hah N, Chi TJ, Tye GL, Armando AM, Evans RM, Chi NW, Quehenberger O, Olefsky JM, Oh DY. Positive reinforcing mechanisms between GPR120 and PPARgamma modulate insulin sensitivity. *Cell Metab* 2020;31:1173–1188 e5.
11. Kimura I, Ichimura A, Ohue-Kitano R, Igarashi M. Free fatty acid receptors in health and disease. *Physiol Rev* 2020;100:171–210.
12. Taylor CT, Colgan SP. Hypoxia and gastrointestinal disease. *J Mol Med (Berl)* 2007;85:1295–1300.
13. Fisher EM, Khan M, Salisbury R, Kuppusamy P. Noninvasive monitoring of small intestinal oxygen in a rat model of chronic mesenteric ischemia. *Cell Biochem Biophys* 2013;67:451–459.
14. Singhal R, Shah YM. Oxygen battle in the gut: hypoxia and hypoxia-inducible factors in metabolic and inflammatory responses in the intestine. *J Biol Chem* 2020;295:10493–10505.
15. Zheng L, Kelly CJ, Colgan SP. Physiologic hypoxia and oxygen homeostasis in the healthy intestine. A review in the theme: cellular responses to hypoxia. *Am J Physiol Cell Physiol* 2015;309:C350–C360.
16. Zeitouni NE, Chotikatam S, von Kockritz-Blickwede M, Naim HY. The impact of hypoxia on intestinal epithelial cell functions: consequences for invasion by bacterial pathogens. *Mol Cell Pediatr* 2016;3:14.
17. Glover LE, Lee JS, Colgan SP. Oxygen metabolism and barrier regulation in the intestinal mucosa. *J Clin Invest* 2016;126:3680–3688.
18. Saeedi BJ, Kao DJ, Kitzenberg DA, Dobrinskikh E, Schwisow KD, Masterson JC, Kendrick AA, Kelly CJ, Bayless AJ, Kominsky DJ, Campbell EL, Kuhn KA, Furuta GT, Colgan SP, Glover LE. HIF-dependent regulation of claudin-1 is central to intestinal epithelial tight junction integrity. *Mol Biol Cell* 2015;26:2252–2262.
19. Karhausen J, Furuta GT, Tomaszewski JE, Johnson RS, Colgan SP, Haase VH. Epithelial hypoxia-inducible factor-1 is protective in murine experimental colitis. *J Clin Invest* 2004;114:1098–1106.
20. Semenza GL. Hypoxia-inducible factors in physiology and medicine. *Cell* 2012;148:399–408.
21. Gonzalez FJ, Xie C, Jiang C. The role of hypoxia-inducible factors in metabolic diseases. *Nat Rev Endocrinol* 2018;15:21–32.
22. Bodnaruc AM, Prud'homme D, Blanchet R, Giroux I. Nutritional modulation of endogenous glucagon-like peptide-1 secretion: a review. *Nutr Metab (Lond)* 2016;13:92.
23. Miyamoto J, Igarashi M, Watanabe K, Karaki SI, Mukouyama H, Kishino S, Li X, Ichimura A, Irie J, Sugimoto Y, Mizutani T, Sugawara T, Miki T, Ogawa J, Drucker DJ, Arita M, Itoh H, Kimura I. Gut microbiota confers host resistance to obesity by metabolizing dietary polyunsaturated fatty acids. *Nat Commun* 2019;10:4007.
24. Ramakrishnan SK, Shah YM. Role of intestinal HIF-2alpha in health and disease. *Annu Rev Physiol* 2016;78:301–325.
25. Singhal R, Mitta SR, Das NK, Kerk SA, Sajjakulnukit P, Solanki S, Andren A, Kumar R, Olive KP, Banerjee R, Lyssiotis CA, Shah YM. HIF-2alpha activation potentiates oxidative cell death in colorectal cancers by increasing cellular iron. *J Clin Invest* 2021;131:e143691.
26. Xie C, Yagai T, Luo Y, Liang X, Chen T, Wang Q, Sun D, Zhao J, Ramakrishnan SK, Sun L, Jiang C, Xue X, Tian Y, Krausz KW, Patterson AD, Shah YM, Wu Y, Jiang C, Gonzalez FJ. Activation of intestinal hypoxia-inducible factor 2alpha during obesity contributes to hepatic steatosis. *Nat Med* 2017;23:1298–1308.
27. Song Y, Koehler JA, Baggio LL, Powers AC, Sandoval DA, Drucker DJ. Gut-proglucagon-derived peptides are essential for regulating glucose homeostasis in mice. *Cell Metab* 2019;30:976–986 e3.
28. Drucker DJ. The role of gut hormones in glucose homeostasis. *J Clin Invest* 2007;117:24–32.
29. Svendsen B, Pedersen J, Albrechtsen NJ, Hartmann B, Torang S, Rehfeld JF, Poulsen SS, Holst JJ. An analysis of cosecretion and coexpression of gut hormones from male rat proximal and distal small intestine. *Endocrinology* 2015;156:847–857.
30. Christensen MB. Glucose-dependent insulinotropic polypeptide: effects on insulin and glucagon secretion in humans. *Dan Med J* 2016;63:B5230.

31. Chan MC, Ilott NE, Schodel J, Sims D, Tumber A, Lippl K, Mole DR, Pugh CW, Ratcliffe PJ, Ponting CP, Schofield CJ. Tuning the transcriptional response to hypoxia by inhibiting hypoxia-inducible factor (HIF) prolyl and asparaginyl hydroxylases. *J Biol Chem* 2016; 291:20661–20673.
32. Keith B, Simon MC. Hypoxia-inducible factors, stem cells, and cancer. *Cell* 2007;129:465–472.
33. Xiong Y, Swaminath G, Cao Q, Yang L, Guo Q, Salomonis H, Lu J, Houze JB, Dransfield PJ, Wang Y, Liu JJ, Wong S, Schwandner R, Steger F, Baribault H, Liu L, Coberly S, Miao L, Zhang J, Lin DC, Schwarz M. Activation of FFA1 mediates GLP-1 secretion in mice. Evidence for allosterism at FFA1. *Mol Cell Endocrinol* 2013;369:119–129.
34. Drucker DJ, Jin T, Asa SL, Young TA, Brubaker PL. Activation of proglucagon gene transcription by protein kinase-A in a novel mouse enteroendocrine cell line. *Mol Endocrinol* 1994;8:1646–1655.
35. Knepel W, Chafitz J, Habener JF. Transcriptional activation of the rat glucagon gene by the cyclic AMP-responsive element in pancreatic islet cells. *Mol Cell Biol* 1990;10:6799–6804.
36. Chang E, Kim L, Choi JM, Park SE, Rhee EJ, Lee WY, Oh KW, Park SW, Park DI, Park CY. Ezetimibe stimulates intestinal glucagon-like peptide 1 secretion via the MEK/ERK pathway rather than dipeptidyl peptidase 4 inhibition. *Metabolism* 2015;64:633–641.
37. Loboda A, Jozkovicz A, Dulak J. HIF-1 and HIF-2 transcription factors—similar but not identical. *Mol Cells* 2010;29:435–442.
38. Kvietys PR, Pittman RP, Chou CC. Contribution of luminal concentration of nutrients and osmolality to postprandial intestinal hyperemia in dogs. *Proc Soc Exp Biol Med* 1976;152:659–663.
39. Jeays AD, Lawford PV, Gillott R, Spencer PA, Bardhan KD, Hose DR. A framework for the modeling of gut blood flow regulation and postprandial hyperaemia. *World J Gastroenterol* 2007;13:1393–1398.
40. Shepherd AP. Metabolic control of intestinal oxygenation and blood flow. *Fed Proc* 1982;41:2084–2089.
41. Matheson PJ, Wilson MA, Garrison RN. Regulation of intestinal blood flow. *J Surg Res* 2000;93:182–196.
42. Ramakrishnan SK, Anderson ER, Martin A, Centofanti B, Shah YM. Maternal intestinal HIF-2 α is necessary for sensing iron demands of lactation in mice. *Proc Natl Acad Sci U S A* 2015;112:E3738–E3747.
43. Xue X, Ramakrishnan S, Anderson E, Taylor M, Zimmermann EM, Spence JR, Huang S, Greenson JK, Shah YM. Endothelial PAS domain protein 1 activates the inflammatory response in the intestinal epithelium to promote colitis in mice. *Gastroenterology* 2013; 145:831–841.
44. Synnestvedt K, Furuta GT, Comerford KM, Louis N, Karhausen J, Eltzschig HK, Hansen KR, Thompson LF, Colgan SP. Ecto-5'-nucleotidase (CD73) regulation by hypoxia-inducible factor-1 mediates permeability changes in intestinal epithelia. *J Clin Invest* 2002; 110:993–1002.
45. Lindgren O, Carr RD, Deacon CF, Holst JJ, Pacini G, Mari A, Ahren B. Incretin hormone and insulin responses to oral versus intravenous lipid administration in humans. *J Clin Endocrinol Metab* 2011;96: 2519–2524.
46. Gribble FM, Reimann F. Function and mechanisms of enteroendocrine cells and gut hormones in metabolism. *Nat Rev Endocrinol* 2019;15:226–237.
47. Hu CJ, Wang LY, Chodosh LA, Keith B, Simon MC. Differential roles of hypoxia-inducible factor 1 α (HIF-1 α) and HIF-2 α in hypoxic gene regulation. *Mol Cell Biol* 2003;23:9361–9374.
48. Ratcliffe PJ. HIF-1 and HIF-2: working alone or together in hypoxia? *J Clin Invest* 2007;117:862–865.
49. Lu VB, Gribble FM, Reimann F. Nutrient-induced cellular mechanisms of gut hormone secretion. *Nutrients* 2021; 13:883.
50. Hira T, Pinyo J, Hara H. What is GLP-1 really doing in obesity? *Trends Endocrinol Metab* 2020;31:71–80.
51. Farhadipour M, Depoortere I. The function of gastrointestinal hormones in obesity—implications for the regulation of energy intake. *Nutrients* 2021;13:1839.
52. Nauck MA, Quast DR, Wefers J, Meier JJ. GLP-1 receptor agonists in the treatment of type 2 diabetes - state-of-the-art. *Mol Metab* 2021;46:101102.
53. Meier JJ. GLP-1 receptor agonists for individualized treatment of type 2 diabetes mellitus. *Nat Rev Endocrinol* 2012;8:728–742.
54. Brunton SA, Wysham CH. GLP-1 receptor agonists in the treatment of type 2 diabetes: role and clinical experience to date. *Postgrad Med* 2020;132(Suppl 2):3–14.
55. Tambuwala MM, Manresa MC, Cummins EP, Aversa V, Coulter IS, Taylor CT. Targeted delivery of the hydroxylase inhibitor DMOG provides enhanced efficacy with reduced systemic exposure in a murine model of colitis. *J Control Release* 2015;217:221–227.
56. Riopel M, Moon JS, Bandyopadhyay GK, You S, Lam K, Liu X, Kisseleva T, Brenner D, Lee YS. Inhibition of prolyl hydroxylases increases hepatic insulin and decreases glucagon sensitivity by an HIF-2 α -dependent mechanism. *Mol Metab* 2020;41:101039.
57. Ramakrishnan SK, Zhang H, Takahashi S, Centofanti B, Periyasamy S, Weisz K, Chen Z, Uhler MD, Rui L, Gonzalez FJ, Shah YM. HIF2 α is an essential molecular brake for postprandial hepatic glucagon response independent of insulin signaling. *Cell Metab* 2016; 23:505–516.
58. Mooli RGR, Rodriguez J, Takahashi S, Solanki S, Gonzalez FJ, Ramakrishnan SK, Shah YM. Hypoxia via ERK signaling inhibits hepatic PPAR α to promote fatty liver. *Cell Mol Gastroenterol Hepatol* 2021; 12:585–597.
59. Mooli RGR, Mukhi D, Watt M, Edmunds L, Xie B, Capooci J, Reslink M, Eze C, Mills A, Stolz DB, Jurczak M, Ramakrishnan SK. Sustained mitochondrial biogenesis is essential to maintain caloric restriction-induced beige adipocytes. *Metabolism* 2020; 107:154225.

Received September 16, 2021. Accepted December 6, 2021.

Correspondence

Address correspondence to: Sadeesh K. Ramakrishnan, PhD, Division of Endocrinology and Metabolism, Department of Medicine, University of Pittsburgh, Pittsburgh, Pennsylvania 15237. e-mail: ramaks@pitt.edu; fax: (412) 648-3290.

CRediT Authorship Contributions

Raja Gopal Reddy Mooli (Conceptualization: Equal; Data curation: Equal; Formal analysis: Equal; Investigation: Equal; Methodology: Equal; Validation: Equal; Visualization: Equal; Writing – original draft: Equal; Writing – review & editing: Equal)

Dhanunjay Mukhi (Data curation: Supporting; Formal analysis: Supporting; Investigation: Supporting; Methodology: Supporting)

Anil K. Pasupulati (Data curation: Supporting; Formal analysis: Supporting; Investigation: Supporting)

Simon Evers (Formal analysis: Supporting; Investigation: Supporting; Methodology: Supporting)

Ian J. Sipula (Data curation: Supporting; Formal analysis: Supporting)

Michael Jurczak (Data curation: Supporting; Formal analysis: Supporting; Supervision: Supporting; Writing – review & editing: Supporting)

Randy J. Seeley (Funding acquisition: Supporting; Supervision: Supporting; Writing – review & editing: Supporting)

Yatrik M. Shah (Conceptualization: Supporting; Formal analysis: Supporting; Funding acquisition: Supporting; Investigation: Supporting; Supervision: Supporting; Writing – review & editing: Supporting)

Sadeesh K. Ramakrishnan (Conceptualization: Lead; Data curation: Lead; Formal analysis: Lead; Funding acquisition: Lead; Investigation: Lead; Methodology: Lead; Supervision: Lead; Writing – original draft: Lead; Writing – review & editing: Lead)

Conflicts of interest

The authors disclose the following: Randy J. Seeley has received grants and personal fees from Novo Nordisk and Astra Zeneca; personal fees from Scobia, Fractyl, and ShouTi Pharma; and holds equity in Calibrate and Rewind. The remaining authors disclose no conflicts.

Funding

This study was funded by the National Institute of Diabetes and Digestive and Kidney Diseases grant DK110537 (S.K.R.); National Institutes of Health grants CA148828, DK095201, and CA245546 (Y.M.S.), and DK117821, DK089503, and DK119188 (R.J.S.); and the Pittsburgh Foundation grant MR2020 109502 (M.J.).